Synthesis, Characterization, and Solution Dynamics of Alkali-Metal Chloride, Aluminate, and Borate Adducts of the Tridentate Amido Diphosphine Ligand Precursor $LiN(SiMe_2CH_2PPr^i_2)_2$

Michael D. Fryzuk,* Garth R. Giesbrecht, and Steven J. Rettig†

Department of Chemistry, University of British Columbia, 2036 Main Mall, Vancouver, British Columbia, Canada V6T 1Z1

Received July 31, 1996⊗

The preparation of LiCl, $LiAlMe_4$, $LiAlEt_4$, $LiBEt_4$, and $NaBEt_4$ adducts of the lithium salt of the potentially tridentate ligand precursor $LiN(SiMe_2CH_2PPr^i_2)_2$ is reported. The reaction of $HN(SiMe_2CH_2Cl)_2$ with $LiPPr^i_2$ (3 equiv) in THF at −78 °C leads to the isolation of $\{LiN(SiMe_2CH_2PPr^i_2)_2\}_2LiCl$, under certain conditions. The X-ray crystal structure shows it to exist as a 2:1 adduct with pseudo C_2 symmetry in which a LiCl molecule is sandwiched between two $LiN(SiMe_2CH_2PPr^i_2)_2$ monomers. The LiCl molecule and two Li−N units form a planar six-membered core which can best be described as a three-rung ladder. The solution ^1H NMR spectrum is consistent with this geometry. Variable-temperature ^{31}P and ^7Li NMR spectroscopy indicate that the basic structural features of this compound are maintained in solution. This is confirmed by a ^7Li NOESY experiment. The addition of $LiAlMe_4$ to $LiN(SiMe_2CH_2PPr^i_2)_2$ results in the formation of $\{LiN(SiMe_2CH_2PPr^i_2)_2{\cdot}LiAlMe_4\}_2$; the same product is formed upon the addition of MeLi (4 equiv) to $AlCl_2[N(SiMe_2CH_2PPr^i_2)_2]$. The X-ray crystal structure of this product indicates that a 2:2 dimer of C_2 symmetry is present. Variable-temperature NMR studies are consistent with a highly fluxional molecule under ambient conditions. The variable-temperature ^6Li NMR spectra of the multiply labeled derivative $\{^6Li^{15}N(SiMe_2CH_2PPr^i_2)_2{\cdot}^6LiAlMe_4\}_2$ indicate that lithium exchange is occurring faster than phosphine exchange. Interaggregate lithium exchange is present under ambient conditions, while at lower temperatures, intraaggregate exchange is more favorable. The behavior of this species varies greatly upon dissolution in coordinating solvents. $LiAlEt_4$ and $LiBEt_4$ adducts of $LiN(SiMe_2CH_2PPr^i_2)_2$ were also formed but could not be crystallized and thus studied in the solid state. The addition of $NaBEt_4$ to $LiN(SiMe_2CH_2PPr^i_2)_2$ affords $\{LiN(SiMe_2CH_2PPr^i_2)_2{\cdot}NaBEt_4\}_x$. The X-ray crystal structure of this compound shows it to be an infinite one-dimensional polymer. In this case, the elucidated structure is the result of aggregation upon solvent evaporation. Comparison of the three crystal structures illustrates that even with varying adducts (i.e., LiCl, $LiAlMe_4$, and $NaBEt_4$) the basic geometries of the $LiN(SiMe_2CH_2PPr^i_2)_2$ unit remain similar.

Introduction

Lithium amide compounds, $LiNR_2$ (R = alkyl, aryl or silyl), have proven to be ubiquitous in organometallic chemistry as amide transfer reagents and also as mild deprotonation reagents for organic synthesis.[1] Recently, in an attempt to better explain the reactivity of organolithium reagents, structural studies have been undertaken to probe the extent and nature of their solvation as well as the degree of aggregation present in solution.[2−15] These studies have revealed a remarkable diversity of bonding types in solution and the solid state, with solvent-separated ion pairs, monomers, dimers, trimers, tetramers, larger oligomers, polymers, ladders, and cages all being known.[1,16−18] What becomes evident from these reports is that the coordination geometry of organolithium reagents is not straightforward and can often vary between the solution and the solid states.

† Experimental Officer: UBC Crystallographic Service.

⊗ Abstract published in *Advance ACS Abstracts,* January 15, 1997.

(1) Sapse, A. M.; Schleyer, P. v. R. *Lithium Chemistry*; Wiley: New York, 1995; p 595.
(2) Reich, H. J.; Gudmundsson, B. Ö. *J. Am. Chem. Soc.* **1996**, *118*, 6074.
(3) Henderson, K. W.; Dorigo, A. E.; Liu, Q.; Williard, P. G.; Schleyer, P. v. R.; Bernstein, P. R. *J. Am. Chem. Soc.* **1996**, *118*, 1339.
(4) Lucht, B. L.; Collum, D. B. *J. Am. Chem. Soc.* **1996**, *118*, 2217.
(5) Lucht, B. L.; Collum, D. B. *J. Am. Chem. Soc.* **1995**, *117*, 9863.
(6) Henderson, K. W.; Walther, D. S.; Williard, P. G. *J. Am. Chem. Soc.* **1995**, *117*, 8680.
(7) Romesberg, F. E.; Collum, D. B. *J. Am. Chem. Soc.* **1994**, *116*, 9198.
(8) Nichols, M. A.; Waldmuller, D.; Williard, P. G. *J. Am. Chem. Soc.* **1994**, *116*, 1153.
(9) Collum, D. B. *Acc. Chem. Res.* **1993**, *26*, 227.
(10) Bernstein, M. P.; Romesberg, F. E.; Fuller, D. J.; Harrison, A. T.; Collum, D. B.; Liu, Q.-Y.; Williard, P. G. *J. Am. Chem. Soc.* **1992**, *114*, 5100.
(11) Romesberg, F. E.; Gilchrist, J. H.; Harrison, A. T.; Fuller, D. J.; Collum, D. B. *J. Am. Chem. Soc.* **1991**, *113*, 5751.
(12) Hall, P. L.; Gilchrist, J. H.; Harrison, A. T.; Fuller, D. J.; Collum, D. B. *J. Am. Chem. Soc.* **1991**, *113*, 9575.
(13) Galiano-Roth, A. S.; Collum, D. B. *J. Am. Chem. Soc.* **1989**, *111*, 6772.
(14) DePue, J. S.; Collum, D. B. *J. Am. Chem. Soc.* **1988**, *110*, 5518.
(15) Williard, T. G.; Salvino, J. M. *Tetrahedron Lett.* **1985**, *26*, 3931.
(16) Mulvey, R. E. *Chem. Soc. Rev.* **1991**, *209*, 167.
(17) Neumann, F.; Hampel, F.; Schleyer, P. v. R. *Inorg. Chem.* **1995**, *34*, 6553.
(18) Gregory, K.; Schleyer, P. v. R.; Snaith, R. *Adv. Inorg. Chem.* **1991**, *37*, 47.

S0276-7333(96)00638-3 CCC: $14.00

Research in our group has been concerned with the use of the lithium amido−diphosphine reagent $LiN(SiMe_2CH_2PR_2)_2$ as a starting material for the introduction of a potentially tridentate ligand to both early and late transition metals and to some main-group elements.[19−26] While this ligand system imbues crystallinity on many of its complexes, the actual lithium precursors have so far not yielded single crystals to allow crystallographic analyses. However, we have been able to isolate and crystallographically characterize LiCl, $LiAlMe_4$, and $NaBEt_4$ adducts of $LiN(SiMe_2CH_2PPr^i_2)_2$, in which three different coordination modes were observed. In this paper we provide details of these solid-state structures and include variable-temperature NMR studies to illustrate that the integrity of these compounds is not always maintained in solution.

Results and Discussion

LiCl Adduct Synthesis. The original preparation of the lithium amido diphosphine reagent $LiN(SiMe_2CH_2PPr^i_2)_2$ requires the addition of 3 equiv of $LiPPr^i_2$ to a THF solution of 1,3-bis(chloromethyl)tetramethyldisilazane (eq 1);[26] 2 equiv of the phosphide is necessary

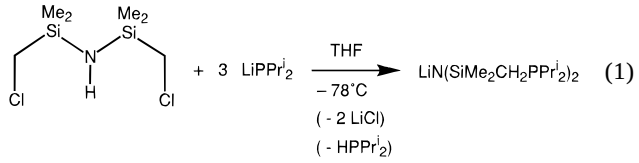

(1)

to displace the chlorides and form the phosphorus−carbon bonds, while the third equivalent deprotonates the amine. The ^1H NMR spectrum consists of peaks attributable to a C_{2v}-symmetric complex with no evidence of any phosphorus−lithium interaction in both the variable-temperature $^{31}P\{^1H\}$ and $^7Li\{^1H\}$ NMR spectra (singlets are observed at all temperatures). The microanalytical data support the above formulation. All of our attempts to grow crystals suitable for X-ray diffraction were foiled, due to the ease with which this compound melts near or slightly above room temperature. However, in one particular preparation, several large colorless crystals could be isolated from a saturated hexanes solution maintained at −40 °C. It became apparent that these crystals, which we label as compound **1** for convenience, were different than the material originally reported on the basis of NMR spectroscopy, elemental analyses, and, most convincingly, X-ray crystallography.

The ^1H NMR spectrum of **1** is nearly identical with that of authentic $LiN(SiMe_2CH_2PPr^i_2)_2$, with the exception that the resonances due to the methylene protons ($-CH_2P$) and the methine protons of the isopropyl groups ($-CH(CH_3)_2$) are noticeably broadened. The $^{31}P\{^1H\}$ NMR spectrum, however, consists of a broad singlet at −3.8 ppm which is indicative of an interaction of phosphorus-31 with a quadrupolar nucleus, in this case lithium-7. This is in contrast to the sharp singlet at −4.7 ppm due to $LiN(SiMe_2CH_2PPr^i_2)_2$. The combustion analysis of the crystals of **1** is consistent with a complex incorporating some degree of LiCl, although it was difficult to determine the exact stoichiometry from the analytical data. Ultimately, an X-ray crystallographic study was necessary to determine the nature of the LiCl interaction in this compound.

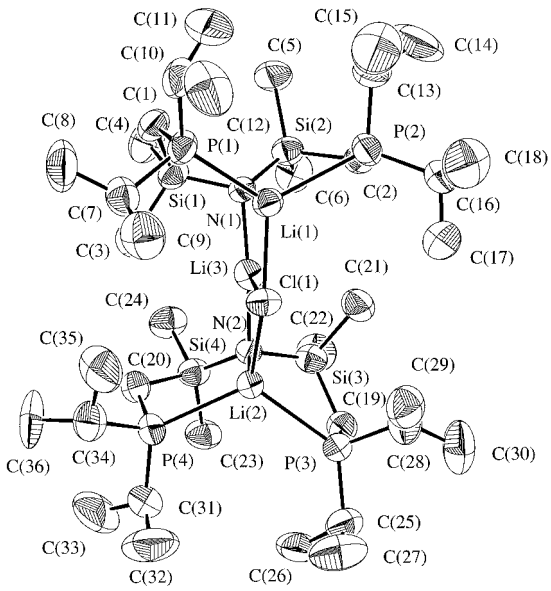

Figure 1. Molecular structure of $\{LiN(SiMe_2CH_2PPr^i_2)_2\}_2$-LiCl (**1**; 33% probability thermal ellipsoids are shown). Hydrogen atoms are omitted for clarity.

Structure of $\{LiN(SiMe_2CH_2PPr^i_2)_2\}_2LiCl$ (1). Cooling a saturated hexanes solution of **1** to −40 °C for 2 weeks resulted in large colorless blocks that were suitable for single-crystal X-ray diffraction. The molecular structure and numbering scheme are illustrated in Figure 1. Complete details of the structural analyses of **1**, **2**, and **6** are presented in Table 1. The structure of **1** can best be described as a three-rung ladder, in which a LiCl unit is sandwiched between two $LiN(SiMe_2CH_2PPr^i_2)_2$ monomers. The formulation of **1** as $\{LiN(SiMe_2CH_2PPr^i_2)_2\}_2LiCl$ is further supported by the microanalytical data. Compound **1** exhibits pseudo C_2 symmetry with the axis passing through the Li(3)−Cl(1) axis. The structural features are similar to those of the four other three-rung ladders of LiCl and two lithium amides previously reported.[3,27,28] **1** contains three lithium atoms in two distinct environments: Li(1) and Li(2) maintain approximate tetrahedral geometries in which bonding to the amide nitrogen and two neutral phosphines of a $LiN(SiMe_2CH_2PPr^i_2)_2$ molecule is observed, in addition to the planar μ_3-chloride associated with LiCl, while Li(2) resides in a distorted-trigonal-planar environment. The bridging lithium Li(2) binds to the chloride and two amido anions. The atoms in the three-rung ladder, Li(1), Cl(1), Li(2), N(2), Li(3), and N(1), define a slightly twisted plane in which the mean

(19) Fryzuk, M. D.; Mylvaganam, M.; Zaworotko, M. J.; MacGillivray, L. R. *Polyhedron* **1996**, *15*, 689.
(20) Fryzuk, M. D.; Gao, X.; Rettig, S. J. *J. Am. Chem. Soc.* **1995**, *117*, 3106.
(21) Fryzuk, M. D.; Giesbrecht, G. R.; Rettig, S. J. *Organometallics* **1996**, *15*, 3329.
(22) Fryzuk, M. D.; Mylvaganam, M.; Zaworotko, M. J.; MacGillivray, L. R. *Polyhedron* **1995**, *15*, 689.
(23) Fryzuk, M. D. *Can. J. Chem.* **1992**, *70*, 2849.
(24) Fryzuk, M. D.; Haddad, T. S.; Berg, D. J.; Rettig, S. J. *Pure Appl. Chem.* **1991**, *63*, 845.
(25) Fryzuk, M. D.; Haddad, T. S.; Rettig, S. J. *Organometallics* **1992**, *11*, 2967.
(26) Fryzuk, M. D.; Carter, A.; Westerhaus, A. *Inorg. Chem.* **1985**, *24*, 642.
(27) Duan, Z.; Young, V. G.; Verkade, J. G. *Inorg. Chem.* **1995**, *34*, 2179.
(28) Mair, F. S.; Clegg, W.; O'Neil, P. A. *J. Am. Chem. Soc.* **1993**, *115*, 3388.

Table 1. Crystallographic Data[a]

compd	{LiN(SiMe$_2$CH$_2$PPr$^i_2$)$_2$}$_2$LiCl, (**1**)	{LiN(SiMe$_2$CH$_2$PPr$^i_2$)$_2$·LiAlMe$_4$}$_2$ (**2**)	{LiN(SiMe$_2$CH$_2$PPr$^i_2$)$_2$·NaBEt$_4$]$_x$ (**6**)
formula	$C_{36}H_{88}ClLi_3N_2P_4Si_4$	$C_{44}H_{112}Al_2Li_4N_2P_4Si_4$	$C_{26}H_{64}BLiNNaP_2Si_2$
fw	841.62	987.35	549.66
cryst syst	monoclinic	triclinic	monoclinic
space group	$P2_1/n$	$P\bar{1}$	$P2_1/c$
a, Å	11.878(2)	16.215(1)	12.519(2)
b, Å	34.137(3)	19.672(1)	35.067(6)
c, Å	13.683(2)	11.5163(9)	17.871(2)
α, deg	90	91.106(7)	90
β, deg	98.98(1)	108.477(6)	109.37(1)
γ, deg	90	100.085(6)	90
V, Å^3	5480(1)	3419.3(5)	7400(1)
Z	4	2	8
ρ_{calc}, g/cm^3	1.020	0.959	0.987
T, °C	21	21	21
radiation	Cu	Cu	Cu
λ, Å	1.541 78	1.541 78	1.541 78
μ, cm^{-1}	27.23	21.21	18.85
transmn factors	0.73−1.00	0.91−1.00	0.88−1.00
$R(F)^a$	0.045	0.056	0.050
$R_w(F)^a$	0.043	0.050	0.041

[a] $R = \Sigma||F_o| - |F_c||/\Sigma|F_o|$; $R_w = (\Sigma w(|F_o| - |F_c|)^2/\Sigma w|F_o|^2)^{1/2}$.

deviation from the plane is 0.1022 Å. Examination of the structure shows that **1** involves a LiCl molecule linking two LiN(SiMe$_2$CH$_2$PPr$^i_2$)$_2$ units together. However, inspection of the structure of **1** reveals four similar lithium−nitrogen bond lengths (2.06(1)−2.10(1) Å) and a lengthened Li(3)−Cl(1) interatomic distance of 2.403(10) Å, which is longer than the distance from the chloride to each of the lithium atoms associated with the LiN(SiMe$_2$CH$_2$PPr$^i_2$)$_2$ units (2.336(10) and 2.333(10) Å). These data reflect the inherent stability of the ladder form in alkali-metal chemistry.[6,12,16,29−31] No unusually short intramolecular contacts were noted. A list of bond lengths and angles for **1** can be found in Table 2.

Variable-Temperature ^{31}P and ^{7}Li NMR Studies of {LiN(SiMe$_2$CH$_2$PPr$^i_2$)$_2$}$_2$LiCl (1). The solution ^{1}H NMR spectrum of **1**, recorded in C_6D_6, is in accord with the structure in the solid state. Each LiN(SiMe$_2$CH$_2$PPr$^i_2$)$_2$ unit possesses local C_{2v} symmetry, and the pseudo mirror plane that is defined by the Li−Cl bond renders each LiN(SiMe$_2$CH$_2$PPr$^i_2$)$_2$ ligand equivalent. The broadened resonances associated with the methylene (SiCH_2P) and methine (PCH(CH$_3$)$_2$) protons reflect a kinetic process in which the phosphine arms rapidly dissociate and recoordinate to the lithium atom bound to the central amide. This postulate is further supported by the variable-temperature ^{31}P{^{1}H} NMR data; at room temperature, a broad singlet at −3.8 ppm is observed for **1**, which upon cooling (in C_7D_8) to −27 °C decoalesces into a 1:1:1:1 quartet at −6.2 ppm. The quartet, a result of coupling to a single quadrupolar lithium-7 nucleus ($I = {}^3/_2$, natural abundance 92.6%), displays a typical $^1J_{P-Li}$ coupling of 48.5 Hz.[32]

At room temperature the ^{7}Li{^{1}H} NMR spectrum also consists of a single broad resonance at −0.7 ppm, even though two distinct lithium environments are present in the solid state. When the temperature is gradually lowered to −38 °C, one observes broadening of the singlet and decoalescence into two resonances of 2:1 intensity: a triplet at −0.4 ppm ($^1J_{P-Li}$ = 48.5 Hz) and a broad singlet at −1.4 ppm (Figure 2). The triplet, which can be attributed to the two lithium ions from the LiN(SiMe$_2$CH$_2$PPr$^i_2$)$_2$ units, coincides with the decoalescence behavior observed in the ^{31}P{^{1}H} spectra, while the broad singlet can be assigned to the lithium bridge between the two amide donors. At first glance, one might conclude that the ^{7}Li{^{1}H} NMR spectra reflect the averaging of the two lithium environments on the NMR time scale, perhaps by lithium site exchange or via the rapid association and dissociation of the phosphine arms to Li(1) and Li(2), as well as Li(3). However, it should be noted that phosphine dissociation cannot by itself average the two environments if the three-rung ladder is maintained in solution. This is illustrated in Scheme 1; if one assumes that the ladder structure is maintained in solution, then phosphine

Table 2. Selected Bond Lengths (Å) and Angles (deg) for {LiN(SiMe$_2$CH$_2$PPr$^i_2$)$_2$}$_2$LiCl (1)

Cl(1)−Li(1)	2.34(1)	Si(1)−N(1)	1.702(4)
Cl(1)−Li(3)	2.40(1)	Si(2)−N(1)	1.687(5)
Cl(1)−Li(2)	2.33(1)	Si(3)−N(2)	1.702(5)
P(1)−Li(1)	2.59(1)	Si(4)−N(2)	1.693(4)
P(2)−Li(1)	2.63(1)	N(1)−Li(1)	2.06(1)
P(3)−Li(2)	2.61(1)	N(1)−Li(3)	2.08(1)
P(4)−Li(2)	2.58(1)	N(2)−Li(2)	2.10(1)
Li(1)−Li(3)	2.79(1)	N(2)−Li(3)	2.10(1)
Li(2)−Li(3)	2.83(1)		
Li(1)−Cl(1)−Li(2)	145.2(4)	Li(2)−Cl(1)−Li(3)	73.2(4)
Li(1)−Cl(1)−Li(3)	72.0(3)	Li(2)−N(2)−Li(3)	84.6(4)
Li(1)−N(1)−Li(3)	84.6(4)	N(1)−Si(1)−C(1)	111.2(2)
N(1)−Si(1)−C(3)	110.2(3)	N(1)−Si(1)−C(4)	116.6(3)
N(1)−Si(2)−C(2)	109.1(2)	N(1)−Si(2)−C(5)	116.2(3)
N(1)−Li(3)−N(2)	161.0(5)	N(1)−Si(2)−C(6)	112.8(3)
N(2)−Si(4)−C(20)	109.4(3)	N(2)−Si(4)−C(23)	114.8(3)
N(2)−Si(4)−C(24)	113.4(3)	P(1)−Li(1)−P(2)	117.9(4)
P(1)−Li(1)−N(1)	97.0(4)	P(2)−Li(1)−N(1)	97.1(4)
P(3)−Li(2)−P(4)	118.9(4)	P(3)−Li(2)−N(2)	95.5(4)
P(4)−Li(2)−N(2)	96.5(4)	Cl(1)−Li(1)−P(1)	114.6(4)
Cl(1)−Li(1)−P(2)	120.4(4)	Cl(1)−Li(1)−N(1)	102.5(4)
Cl(1)−Li(2)−P(3)	116.7(4)	Cl(1)−Li(2)−P(4)	118.8(4)
Cl(1)−Li(2)−N(2)	101.7(4)	Cl(1)−Li(3)−N(1)	99.5(4)
Cl(1)−Li(3)−N(2)	99.5(4)	Si(1)−N(1)−Si(2)	122.7(3)
Si(1)−N(1)−Li(1)	107.2(4)	Si(1)−N(1)−Li(3)	106.9(4)
Si(2)−N(1)−Li(1)	110.7(4)	Si(2)−N(1)−Li(3)	117.8(4)
Si(3)−N(2)−Si(4)	122.1(3)	Si(3)−N(2)−Li(2)	107.3(3)
Si(3)−N(2)−Li(3)	106.2(4)	Si(4)−N(2)−Li(2)	110.1(3)
Si(4)−N(2)−Li(3)	119.7(4)		

(29) Gardiner, M. G.; Raston, C. L. *Inorg. Chem.* **1995**, *34*, 4206.
(30) Armstrong, D. R.; Barr, D.; Clegg, W.; Mulvey, R. E.; Reed, D.; Snaith, R.; Wade, K. *J. Chem. Soc., Chem. Commun.* **1986**, 869.
(31) Armstrong, D. R.; Barr, D.; Clegg, W.; Hodgson, S. M.; Mulvey, R. E.; Reed, D.; Snaith, R.; Wright, D. S. *J. Am. Chem. Soc.* **1989**, *111*, 4719.
(32) Fryzuk, M. D.; Love, J. B.; Rettig, S. J. *J. Chem. Soc., Chem. Commun.*, in press.

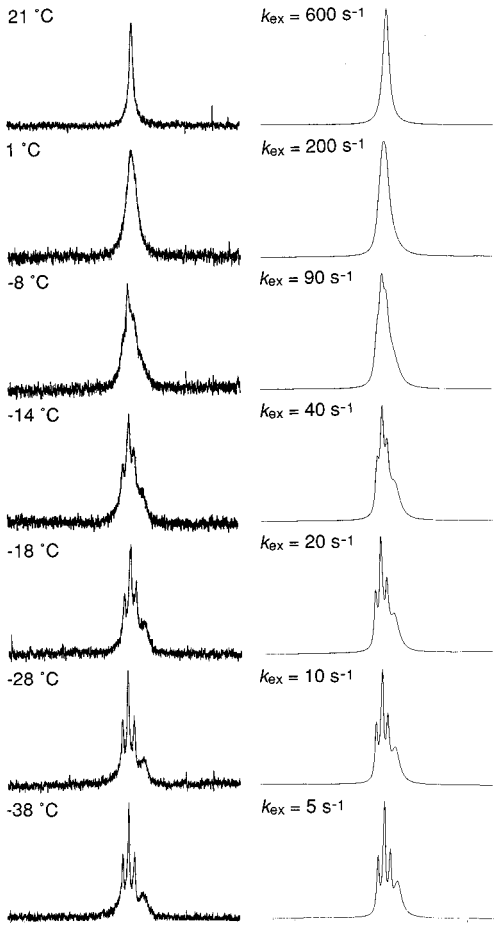

Figure 2. Experimental (left) and simulated (right) variable-temperature ^{7}Li{^{1}H} spectra of {LiN(SiMe$_2$CH$_2$PPr$^i_2$)$_2$}$_2$-LiCl (**1**) in C_7D_8.

migration from one type of lithium to the other never exchanges the two different lithium environments present. This was confirmed by the ^{7}Li NOESY spectrum of the ^{15}N-labeled derivative {Li^{15}N(SiMe$_2$CH$_2$-PPr$^i_2$)$_2$}$_2$LiCl, (**1b**) run in C_7D_8 at −50 °C. As shown in Figure 3, no off-diagonal peaks were observed upon varying t_{mix} from 5 to 50 ms, which in previous work was found to be sufficient for observing dynamic processes in the slow-exchange limit for analogous systems.[33−35] The low-temperature ^{7}Li NOESY illustrates that lithium site exchange does not occur to any appreciable extent and that the structural integrity of **1** is retained in solution. Other LiCl adducts such as {(μ_3-Cl)Li$_3$H$_4$[(Me$_3$SiNCH$_2$CH$_2$)$_3$N]$_2$} also retain their structural integrity even up to 65 °C.[27]

From the variable-temperature ^{7}Li{^{1}H} NMR data, we were able to derive kinetic parameters regarding the *apparent* exchange of three lithium atoms over two sites: from the Arrhenius plot, $\Delta G_{T_c}^{\ddagger}$, $\Delta H^{\ddagger}$, and $\Delta S^{\ddagger}$ were determined to be 13.2 kcal/mol, 11.2 kcal/mol, and −7 ± 8 cal/(K/mol), respectively. The value of $\Delta S^{\ddagger}$, although small and subject to considerable error, is further evidence of the retention of the ladder conformation in solution and complements the ^{7}Li NOESY results. If the positions of the lithium atoms in **1** were exchanged

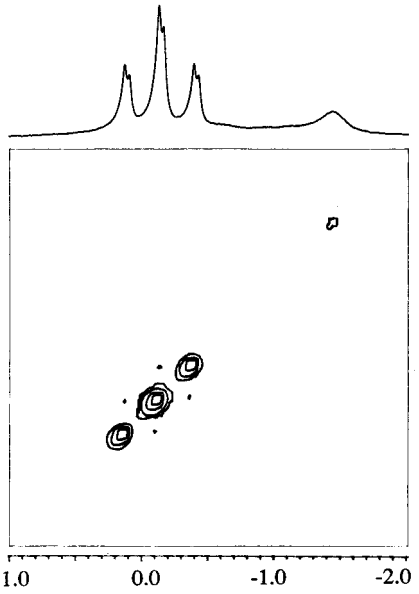

Figure 3. ^{7}Li NOESY spectrum of {Li^{15}N(SiMe$_2$CH$_2$-PPr$^i_2$)$_2$}$_2$LiCl (**1b**) in C_7D_8 at 223 K. The small coupling present is due to ^{7}Li−^{15}N coupling ($^1J_{Li-^{15}N}$ = 5.8 Hz).

Scheme 1

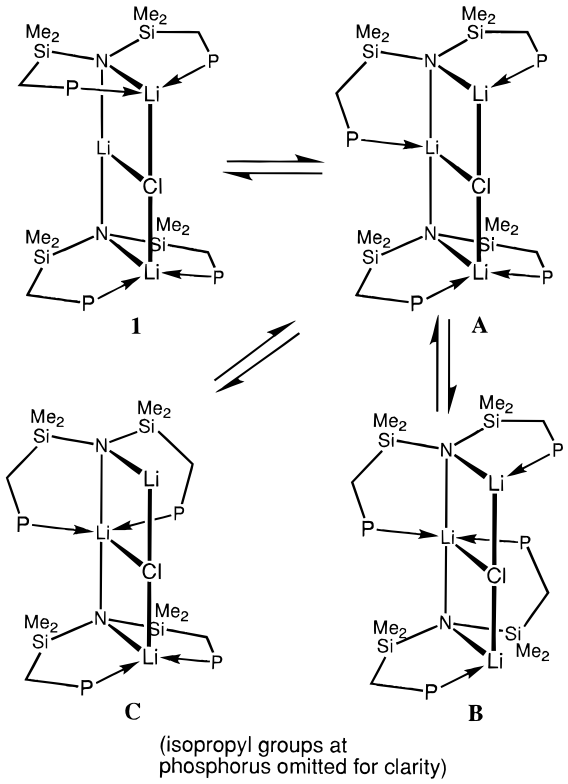

by a process whereby the ladder structure was lost, one would expect a much different value for $\Delta S^{\ddagger}$. That the lithium environments are averaged by a nonintrusive mechanism such as phosphine dissociation and recoordination is supported by the minimal value determined for $\Delta S^{\ddagger}$.

Still, the fact remains that at the high-temperature limit of the variable-temperature ^{7}Li{^{1}H} NMR spectra (Figure 2), a broadened singlet is observed. This is unusual for two reasons: (i) there should be two environments for the two different types of lithiums present in the ladder structure even at high temperature, and (ii) the coupling information from the phos-

(33) Arnold, J. *J. Chem. Soc., Chem. Commun.* **1990**, 976.
(34) Arnold, J.; Dawson, D. Y.; Hoffman, C. G. *J. Am. Chem. Soc.* **1993**, *115*, 2707.
(35) Briere, K. M.; Dettman, H. D.; Detellier, C. *J. Magn. Reson.* **1991**, *94*, 600.

phorus-31 nuclei has been lost. To rationalize the apparent observation of only one environment, we suggest that this is a result of the phosphine exchange process and the relatively small chemical shift range for ^{7}Li. As shown in Scheme 1, in the fast exchange limit, each lithium can be found with two, one, or no coordinated phosphine ligands. Given the ionic nature of lithium compounds, and the fact that the small chemical shift range for lithium-7 is not that sensitive to environmental changes, the apparent observation of a single environment in the high-temperature limit is reasonable. The other unusual aspect is that this resonance appears as a *singlet*; in other words, coupling information from the phosphorus-31 nuclei has been lost. For a purely intramolecular process that involves fast phosphine dissociation and reassociation, coupling information should still be present, albeit statistically weighted to reflect residence time. However, in this case, because ^{7}Li is quadrupolar, as the temperature is raised quadrupolar relaxation becomes fast with respect to J_{LiP}, resulting in the formation of a singlet and not the expected triplet.[36]

We undertook other heteronuclear NMR spectroscopic studies on **1** in hopes of further confirming that the structure determined in the solid state was also indicative of its solution geometry. The ^{29}Si{^{1}H} NMR spectrum of the labeled derivative {Li^{15}N(SiMe$_2$CH$_2$PPr$^i_2$)$_2$}$_2$LiCl (**1b**) exhibited only a broad singlet (δ −17.2 ppm), which can be viewed as indicative of either a compound with C_{2v} symmetry or a fluxional process on the NMR time scale. Similar results were garnered from the ^{15}N{^{1}H} NMR spectra, which maintained sharp singlets at both room temperature and −50 °C (δ 5.1 ppm). The lack of coupling from ^{15}N to ^{7}Li in the ^{15}N{^{1}H} NMR spectra is expected on the basis of the quadrupolar moment of ^{7}Li.[37] However, the ^{7}Li{^{1}H} NMR spectrum obtained at −50 °C (194.4 MHz) exhibited a small $^1J_{Li-^{15}N}$ coupling of 5.8 Hz. Even though we were unable to obtain a suitable solution molecular weight measurement of **1** (via the Signer method), we conclude that the NMR spectroscopic data indicate that the basic structural features of **1** are maintained in solution, and the crystal structure determined is not merely a chance feature of aggregation.

Mechanism of Formation of {LiN(SiMe$_2$CH$_2$PPr$^i_2$)$_2$}$_2$LiCl (1). The serendipitous discovery of **1** may be the result of incomplete removal of THF from the original reaction mixture. We suggest that the presence of small quantities of THF serves to both solubilize the LiCl coproduct and solvate the lithium amide unit, presumably in a dimeric form. Although an early report suggested that structures such as **1** arose from the trapping of a LiCl molecule by two lithium amide monomers,[28] recent work argues that three-rung ladders are a result of the incorporation of a LiCl molecule into an open (R$_2$NLiS$_x$)$_2$ dimer.[3,15,38] One can also generate **1** from the addition of LiCl to LiN(SiMe$_2$CH$_2$PPr$^i_2$)$_2$ (2 equiv) in either THF or toluene; the resultant crystalline solids exhibited ^{1}H and ^{31}P{^{1}H} NMR spectra identical with those for **1**, although no attempt was made to further analyze them. The three-rung ladder structure of **1** does not hinder further metathesis chemistry, however, as reaction with metal halides MX$_{n+1}$ results in the expected MX$_n$[N(SiMe$_2$CH$_2$PPr$^i_2$)$_2$] products (e.g., AlCl$_3$ and ScCl$_3$[21,39]).

Scheme 2

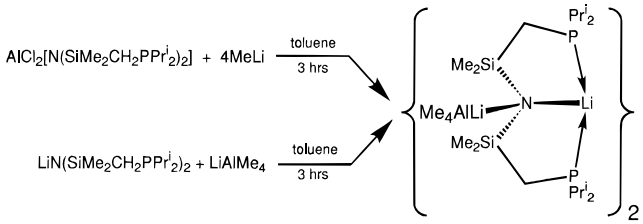

2

As a final note, we should clarify that the original preparation[26] of LiN(SiMe$_2$CH$_2$PPr$^i_2$)$_2$ is accurate as long as all the THF from the preparation is removed before extraction of the product with hexanes; in this way, all of the LiCl precipitates and formation of the LiCl adduct **1** is prevented.

LiAlMe$_4$ Adduct Synthesis. While examining the reaction chemistry of aluminum derivatives of the general formula AlR$_2$[N(SiMe$_2$CH$_2$PPr$^i_2$)$_2$] (R = Cl, Me, Et, Bz),[39] we serendipitously discovered the formation of yet another adduct of LiN(SiMe$_2$CH$_2$PPr$^i_2$)$_2$. Upon the addition of 4 equiv of MeLi to the starting aluminum dichloride, AlCl$_2$[N(SiMe$_2$CH$_2$PPr$^i_2$)$_2$], we obtained a clear colorless oil that could be crystallized from toluene. The ^{1}H NMR spectrum of this compound exhibits characteristic ligand backbone resonances in addition to a large singlet at −0.21 ppm that corresponds to 12 protons. The upfield position of this peak, and the absence of a triplet in the same vicinity (due to 6 methyl protons coupling to two equivalent phosphorus-31 nuclei, as is found for AlMe$_2$[N(SiMe$_2$CH$_2$PPr$^i_2$)$_2$][39]), points toward an aluminate type structure. Also, the ^{31}P{^{1}H} NMR spectrum consists of only a single sharp peak at −3.5 ppm. Previously, we have found that phosphine resonances bound to quadrupolar nuclei (i.e., ^{45}Sc, I = $^7/_2$; ^{27}Al, I = $^5/_2$) display broadened resonances in the absence of fast exchange.[21,39] The elemental microanalysis of this product is also consistent with the empirical formulation LiN(SiMe$_2$CH$_2$PPr$^i_2$)$_2$·LiAlMe$_4$ (**2**). Additionally, if LiN(SiMe$_2$CH$_2$PPr$^i_2$)$_2$ is added to a slurry of LiAlMe$_4$ (1 equiv) in toluene, a product exhibiting identical ^{1}H, ^{31}P{^{1}H}, and ^{7}Li{^{1}H} NMR spectra is obtained (Scheme 2). All of these factors point toward **2** as being a LiAlMe$_4$ adduct of LiN(SiMe$_2$CH$_2$PPr$^i_2$)$_2$. The isolation of crystals allowed us to undertake a structural study of **2** and to show that it has a dimeric molecular formulation.

Structure of {LiN(SiMe$_2$CH$_2$PPr$^i_2$)$_2$·LiAlMe$_4$}$_2$ (2). Evaporation of a saturated toluene solution of **2** resulted in large colorless plates that were suitable for single-crystal X-ray diffraction. The molecular structure and numbering scheme are illustrated in Figure 4. The structure is made up of two LiN(SiMe$_2$CH$_2$PPr$^i_2$)$_2$·LiAlMe$_4$ units which form a dimer with C_2 symmetry. Each $^-$N(SiMe$_2$CH$_2$PPr$^i_2$)$_2$ ligand chelates a lithium cation in a geometry intermediate between facial and meridional. The coordination of each $^-$N(SiMe$_2$CH$_2$-

(36) Harris, R. K. *Nuclear Magnetic Resonance Spectroscopy*; Pitman Books: London, 1983; p 187.
(37) Brand, H.; Capriotti, J. A.; Arnold, J. *Inorg. Chem.* **1994**, *33*, 4334.
(38) Romesberg, F. E.; Collum, D. B. *J. Am. Chem. Soc.* **1994**, *116*, 9187.
(39) Fryzuk, M. D.; Giesbrecht, G. R.; Olovsson, G.; Rettig, S. J. *Organometallics* **1996**, *15*, 4832.

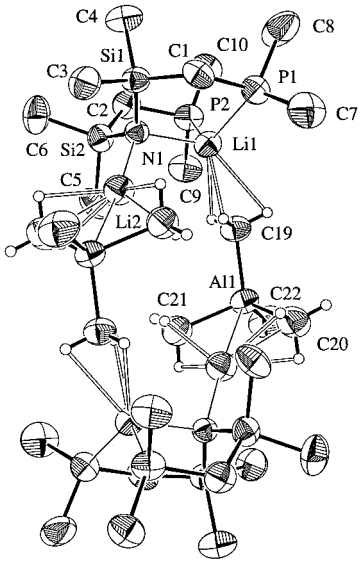

Figure 4. Molecular structure of $\{LiN(SiMe_2CH_2PPr^i_2)_2 \cdot LiAlMe_4\}_2$ (**2**; 33% probability thermal ellipsoids are shown). Hydrogen atoms are omitted for clarity.

$PPr^i_2)_2$ ligand to lithium rather than an aluminum is noteworthy, particularly since aluminum was the central metal in the starting material. Each lithium in the dimer maintains a roughly tetrahedral geometry: Li(1) is coordinated by two phosphines of a $^-N(SiMe_2CH_2PPr^i_2)_2$ ligand and an amide, in addition to a carbon associated with a bridging $^-AlMe_4$ unit. The greatest deviation from ideal is evident in the P(1)−Li(1)−P(2) angle of 124.1(3)° and the two P−Li(1)−N(1) angles of 96.3(3) and 96.9(3)°. The phosphorus−lithium bond lengths of 2.538(7) and 2.675(7) Å in **2** are both similar to those found in **1**. The distances determined between lithium and both nitrogen and carbon are well within normal values associated with these types of bonds. The second lithium atom resides in a much less conventional geometry: Li(2) shares short contacts with the same amide as Li(1), two carbons, three hydrogens, and an aluminum atom. The distorted environment around the Li(2) atom is also apparent in an almost linear N(1)−Li(2)−Al(1′) angle of 164.6(4)°. If one discounts the contacts present with three hydrogens (two on C(20) and one on C(21)), Li(2) can be said to reside in a greatly distorted tetrahedral environment, in which the two carbon atoms and the aluminum atom are greatly bent back from the Li(2)−N(1) bond. It may be that the steric bulk of the silyl methyl groups of the $^-N(SiMe_2CH_2PPr^i_2)_2$ ligand prevents a more ideal geometry from being attained. It is well-known that the environment of the small lithium cation is governed primarily by steric factors.[1,40] The bridging tetrahedral $^-AlMe_4$ groups present no unusual bond angles or bond lengths. A partial list of bond lengths and bond angles for **2** are presented in Table 3.

Variable-Temperature NMR Studies of $\{LiN(SiMe_2CH_2PPr^i_2)_2 \cdot LiAlMe_4\}_2$ (2). The fluxional behavior of $\{LiN(SiMe_2CH_2PPr^i_2)_2 \cdot LiAlMe_4\}_2$ was studied by variable-temperature NMR spectroscopy. All of the methyl groups of the tetramethylaluminate moiety were found to be equivalent, since the resonance corresponding to these protons (^{1}H NMR spectra) remained a singlet down to the solvent limit (−90 °C, C_7D_8), with no coupling to phosphorus or lithium being observed. The shift of this resonance was also found to be solvent-dependent (−0.21 ppm in C_6D_6, −0.38 ppm in C_7D_8), which is perhaps indicative that the $^-AlMe_4$ group is mobile in solution. Previous work with lithium amides has shown that the quadrupolar interactions present (^{7}Li, ^{14}N) often prevent well-defined spectra from being attained.[4,5,7−14] Thus, we performed $^{31}P\{^1H\}$, $^6Li\{^1H\}$, and $^{15}N\{^1H\}$ NMR experiments on the labeled derivative $\{^6Li^{15}N(SiMe_2CH_2PPr^i_2)_2 \cdot {}^6LiAlMe_4\}_2$ (**2b**), which was synthesized in a fashion analogous to that for **2** from $AlCl_2[^{15}N(SiMe_2CH_2PPr^i_2)_2]$ and $CH_3{}^6Li$.

The $^{31}P\{^1H\}$ NMR spectra of **2b** experienced no change as the temperature was lowered from 20 to −88 °C in C_7D_8; the sharp singlet present at room temperature persisted at all temperatures and shifted upfield to −8.6 ppm (from −3.5 ppm) at the low-temperature limit. This behavior is analogous to that observed for a series of aluminum dialkyls of this ligand system, which we have attributed to the highly fluxional character of electropositive main-group compounds of $N(SiMe_2CH_2PPr^i_2)_2$.[39] The room-temperature $^6Li\{^1H\}$ NMR spectrum of **2b** in C_7D_8/pentane is also a sharp singlet (δ 1.4 ppm) (Figure 5). When the temperature is lowered to −48 °C, the singlet gradually broadens and evolves into a triplet of doublets at 1.2 ppm ($^1J_{^6Li-P}$ = 10.8 Hz, $^1J_{^6Li-^{15}N}$ = 3.2 Hz) due to the coupling of both lithium atoms to two phosphines and a single ^{15}N nucleus (I = $^1/_2$). In this intermediate temperature regime, the presence of only one multiplet is consistent

Table 3. Selected Bond Lengths (Å) and Angles (deg) for $\{LiN(SiMe_2CH_2PPr^i_2)_2 \cdot LiAlMe_4\}_2$, (2)[a]

Al(1)−C(19)	1.988(4)	Al(1)−C(20)	2.012(5)
Al(1)−C(21)	2.024(5)	Al(1)−Li(2′)	2.736(8)
Al(1)−C(22)	1.964(5)	Al(2)−C(43)	2.008(6)
Al(2)−C(41)	1.992(4)	Al(2)−C(42)	2.006(5)
Al(2)−C(43)	2.008(6)	Al(2)−C(44)	1.976(6)
Al(2)−Li(4″)	2.714(8)	P(1)−Li(1)	2.538(7)
P(2)−Li(1)	2.675(7)	P(3)−Li(3)	2.656(7)
P(4)−Li(3)	2.556(7)	N(1)−Li(1)	2.075(8)
N(1)−Li(2)	1.988(9)	N(2)−Li(3)	2.076(8)
N(2)−Li(4)	1.989(8)	Li(1)−H(46)	2.47
Li(1)−H(47)	2.19	Li(1)−H(45)	2.19
Li(2)−H(48′)	2.10	Li(2)−H(49′)	2.15
Li(2)−H(53′)	2.08	Li(2)−H(52′)	2.08
Li(3)−H(100)	2.38	Li(3)−H(102)	2.26
Li(3)−H(101)	2.27	Li(4)−H(107)″	2.08
Li(4)−H(105)″	2.09	Li(4)−H(103)″	2.10
Li(4)−H(106)″	2.07	Si(1)−N(1)	1.698(3)
Si(2)−N(1)	1.707(3)	Si(3)−N(2)	1.697(3)
Si(4)−N(2)	1.709(3)	C(20)−Li(2′)	2.31(1)
C(21)−Li(2′)	2.270(9)	C(42)−Li(4)″	2.28(1)
C(43)−Li(4)″	2.261(9)		
Si(1)−N(1)−Li(1)	109.9(2)	Si(1)−N(1)−Li(2)	105.1(3)
Si(2)−N(1)−Li(1)	104.8(2)	Si(2)−N(1)−Li(2)	106.2(3)
Si(1)−N(1)−Si(2)	123.0(2)	Si(4)−N(2)−Li(4)	105.3(3)
Si(3)−N(2)−Li(3)	105.3(3)	Si(3)−N(2)−Si(4)	123.7(2)
Si(3)−N(2)−Li(4)	107.5(3)	Si(4)−N(2)−Li(3)	108.5(2)
P(1)−Li(1)−P(2)	124.1(3)	P(1)−Li(1)−N(1)	96.9(3)
P(2)−Li(1)−N(1)	96.3(3)	P(3)−Li(3)−N(2)	96.3(3)
P(3)−Li(3)−P(4)	123.9(3)	P(4)−Li(3)−N(2)	97.7(3)
Li(1)−N(1)−Li(2)	107.1(3)	Li(3)−N(2)−Li(4)	105.2(3)
N(1)−Si(1)−C(1)	109.7(2)	N(1)−Si(2)−C(2)	111.8(2)
N(1)−Si(1)−C(3)	112.4(2)	N(1)−Si(2)−C(5)	109.5(2)
N(1)−Si(1)−C(4)	115.5(2)	N(1)−Si(2)−C(6)	114.7(2)
N(2)−Si(3)−C(23)	111.3(2)	N(2)−Si(3)−C(25)	114.9(2)
N(2)−Si(3)−C(26)	110.5(2)	N(2)−Si(4)−C(24)	109.7(2)
N(2)−Si(4)−C(27)	116.0(2)	N(2)−Si(4)−C(28)	112.5(2)

[a] Symbols refer to symmetry operations: (′) $1-x, 1-y, -z$; (″) $2-x, -y, 1-z$.

(40) Schade, C.; Schleyer, P. v. R. *Adv. Organomet Chem* **1988**, *27*, 169.

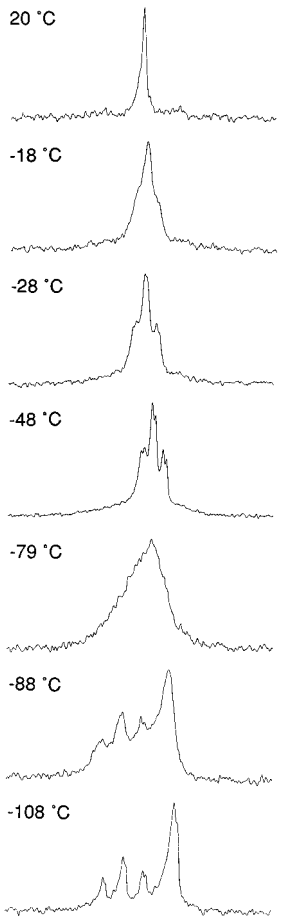

Figure 5. Variable-temperature ^{6}Li{^{1}H} spectra of {^{6}Li^{15}N(SiMe$_2$CH$_2$PPr$^i_2$)$_2$·^{6}LiAlMe$_4$}$_2$ (**2b**) in C$_7$D$_8$/pentane.

with fast lithium exchange between the two equivalent sites. Further cooling (−78 °C) results in the loss of all coupling information to regenerate a broad singlet. Finally, at −108 °C, two resonances of equal intensity are evident: a triplet of doublets at 1.9 ppm ($^1J_{^6\mathrm{Li}-\mathrm{P}}$ = 19.9 Hz, $^1J_{^6\mathrm{Li}-^{15}\mathrm{N}}$ = 2.0 Hz) due to a lithium bound to two phosphines and an amide of a ^{15}N(SiMe$_2$CH$_2$PPr$^i_2$)$_2$ ligand and a doublet at 0.7 ppm ($^1J_{^6\mathrm{Li}-^{15}\mathrm{N}}$ = 4.0 Hz) arising from a lithium atom bound only to the amide nitrogen. Thus, the low-temperature ^{6}Li{^{1}H} NMR spectrum of **2b** is similar to that of **1** and is in accord with the solid-state structure, in which two distinct lithium environments were determined. However, the solution data are also consistent with the monomeric adduct LiN(SiMe$_2$CH$_2$PPr$^i_2$)$_2$·LiAlMe$_4$. From the decoalescence behavior of **2b** between −78 and −108 °C, the following activation parameters were determined: $\Delta G_{\mathrm{Tc}}^{\ddagger}$ = 9.3 kcal/mol, $\Delta H^{\ddagger}$ = 8.4 kcal/mol, and $\Delta S^{\ddagger}$ = −4 ± 8 cal/(K/mol). The similarity of these values to those determined for the chloride adduct **1** suggest that the mechanism of lithium exchange in this low-temperature range is also a result of phosphine dissociation and reassociation. Such a process is outlined in Scheme 3.

As mentioned above, the variable-temperature ^{6}Li{^{1}H} NMR spectra point toward a monomeric form being present at most temperatures in solution. Additional support for this comes from the room-temperature solution molecular weight determination (Signer method) of **2b**, which corresponds to a simple 1:1 LiAlMe$_4$ adduct of LiN(SiMe$_2$CH$_2$PPr$^i_2$)$_2$. Since the dimer is held together in the solid state by two relatively weak interactions that involve only one methyl group of the aluminate moiety and the lithium bound to the phosphine donors, the formation of the monomeric form **D** is reasonable (Scheme 3). At room temperature, the molecule is highly fluxional, with rapidly dissociating phosphines and exchanging lithium centers. When the temperature is lowered to −48 °C, rapid lithium exchange is still occurring, although coupling to phosphorus-31 and nitrogen-15 is evident. To exchange the lithiums, a symmetrical intermediate such as **E** can be envisioned since it would involve dissociation of one arm of the ligand from one Li and recoordination to the other concomitant with the AlMe$_4$ moiety bridging the two lithiums. Cycling through structures **D**, **E**, and **D′** provides the necessary pathway to exchange the lithium centers as well as the methyls on Al. The ^{6}Li{^{1}H} NMR spectrum at −108 °C indicates that two lithium types are present, one of them not exhibiting lithium−phosphorus coupling and therefore consistent with the monomeric form **D** or **D′** in the slow exchange limit.

It should be pointed out that the fluxional process detailed in Scheme 3 is only applicable to the temperature regime below −48 °C; above this temperature, loss of coupling from ^{6}Li to both ^{15}N and ^{31}P is observed, which suggests that an *intermolecular* process becomes operative that exchanges lithium centers. One possibility is dissociation of the monomeric unit **D** or **D′** into LiAlMe$_4$ and LiN(SiMe$_2$CH$_2$PPr$^i_2$)$_2$. In contrast to that previously discussed for the ladder structure of **1**, the loss of coupling for **2b** at higher temperatures is not due to quadrupolar relaxation. Because **2b** is the lithium-6-labeled material, the lower quadrupolar moment of ^{6}Li (I = 1, −0.0008 b) as compared to ^{7}Li (I = $^3/_2$, −0.04 b), used in **1**, effectively removes this as a mechanism for relaxation.

The results of the ^{29}Si{^{1}H} and ^{15}N{^{1}H} NMR studies were similar to those found for the labeled lithium chloride adduct **1b**. The ^{29}Si{^{1}H} NMR spectrum of **2b** consists of a singlet at −18.5 ppm, which again is consistent with a highly symmetric molecule (as in the crystal structure of **2**) or a highly fluxional molecule. The ^{15}N{^{1}H} NMR spectra at ambient temperature (δ 27.3 ppm) and at −108 °C both showed no ^{15}N−^{6}Li coupling.

The behavior of **2** was found to vary greatly upon dissolution in coordinating solvents. In the ^{1}H NMR spectrum in THF-d_8, the $^-$AlMe$_4$ resonance, a singlet at −0.21 ppm in C$_6$D$_6$, becomes a 1:1:1:1:1:1 sextet at −1.36 ppm, which does not change upon ^{31}P decoupling. This pattern, due to aluminum−proton coupling ($^2J_{\mathrm{H}-\mathrm{Al}}$ = 6.1 Hz) is indicative of a very symmetric environment around the Al nucleus and is identical in shift and coupling with that of a THF-d_8 solution of LiAlMe$_4$. The resonances due to LiN(SiMe$_2$CH$_2$PPr$^i_2$)$_2$ are shifted slightly upfield and sharpened considerably. As with LiAlMe$_4$, these resonances are analogous to those of a simple THF-d_8 solution of LiN(SiMe$_2$CH$_2$PPr$^i_2$)$_2$. From these data, one can conclude that coordinating solvents such as THF break up the adduct, resulting in what is likely three discrete species in solution, as has been observed for other lithium amides.[41] The ^{6}Li{^{1}H} NMR spectrum of **2b** in THF-d_8 was comprised of a singlet at 0.1 ppm, which most likely reflects an averaged signal

(41) Gade, L. H.; Mahr, N. *J. Chem. Soc., Dalton. Trans.* **1993**, 489.

Scheme 3

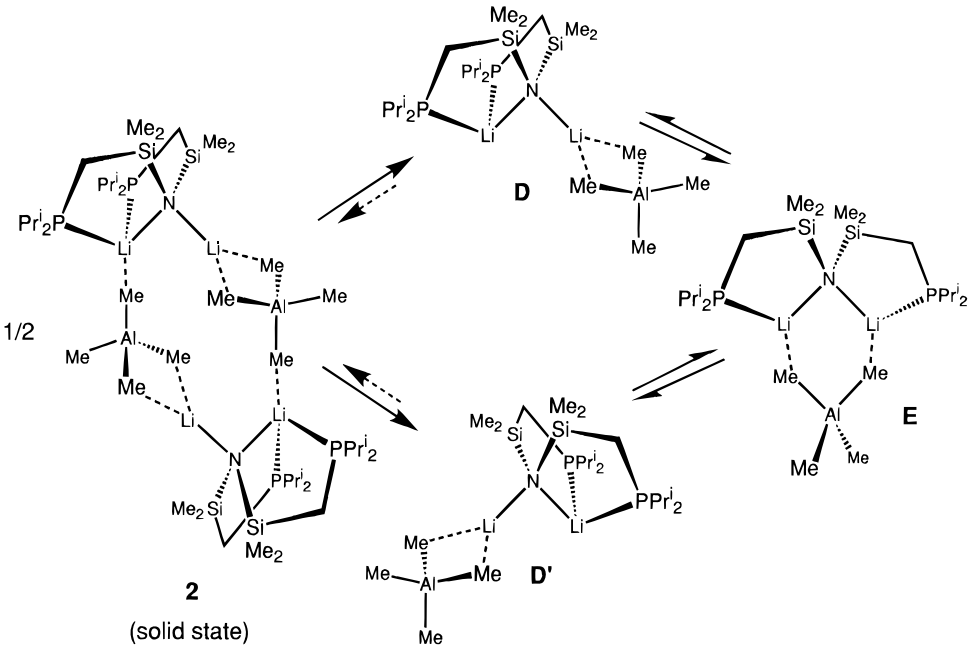

Scheme 4

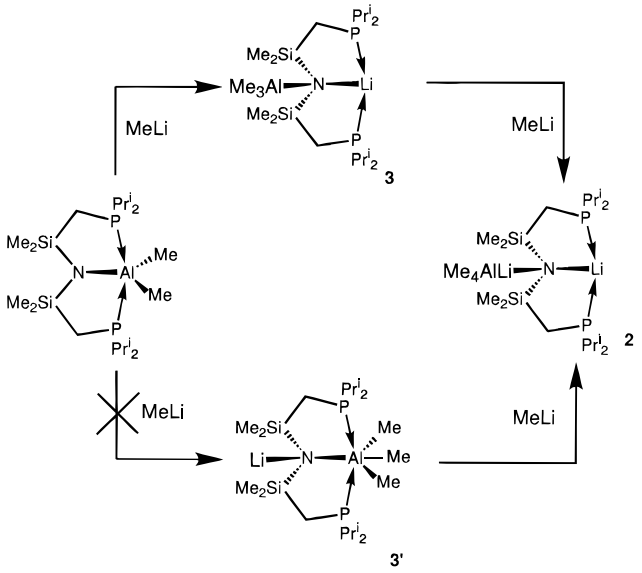

from both $LiN(SiMe_2CH_2PPr^i_2)_2$ and $[Li(THF)_x]^+[AlMe_4]^-$. We did not probe the nature of this exchange any further.

Mechanism of Formation of $\{LiN(SiMe_2CH_2PPr^i_2)_2{\cdot}LiAlMe_4\}_2$ (2). The formation of a lithium aluminate adduct of $LiN(SiMe_2CH_2PPr^i_2)_2$ upon reaction of $AlCl_2[N(SiMe_2CH_2PPr^i_2)_2]$ with 4 equiv of MeLi may be rationalized if one allows for the insertion/addition of MeLi into/across the aluminum−amide bond. As previously reported, the first 2 equiv of MeLi forms the dimethyl complex $AlMe_2[N(SiMe_2CH_2PPr^i_2)_2]$; the third equivalent of MeLi then either inserts into the aluminum−amide bond to form **3** or adds across the aluminum−amide bond to form **3′** (Scheme 4). The fourth equivalent of MeLi then results in the formation of the product **2**. In either case, the final product is the result of an aluminum atom being displaced from the $^-N(SiMe_2CH_2PPr^i_2)_2$ coordination sphere in favor of lithium. To test our hypothesis, we added 3 equiv of MeLi to the starting dichloride. The product obtained showed ^1H NMR resonances for a singlet corresponding to nine protons at −0.30 ppm and a sharp singlet in the $^{31}P\{^1H\}$ NMR spectrum at −4.0 ppm; these data are best rationalized using structure **3** as the intermediate rather than **3′**, since the latter would be expected to exhibit a methyl resonance with phosphorus-31 coupling in the ^1H NMR spectrum and a broadened $^{31}P\{^1H\}$ NMR spectrum due to the presence of aluminum-27. We have previously suggested a structure similar to **3** in earlier iridium amido diphosphine chemistry.[42] Although no resonances indicative of the alternative structure **3′** were evident, the initial formation of this complex and its rapid conversion to **3** cannot be ruled out.

$LiAlEt_4$, $LiBEt_4$, and $NaBEt_4$ Adduct Synthesis. The ease with which we were able to generate a lithium aluminate adduct of $LiN(SiMe_2CH_2PPr^i_2)_2$ by the addition of $LiAlMe_4$ prompted us to examine the potential of other alkali-metal metalates as complexing agents. Thus, toluene solutions of $LiN(SiMe_2CH_2PPr^i_2)_2$ were added to slurries of $LiAlEt_4$, $LiBEt_4$, and $NaBEt_4$ in toluene to examine the effect of the systematic variation of the cation (Li to Na), the tripositive metal of the anion (Al to B), and the alkyl group present (Me to Et). In all three cases, addition of the ligand system resulted in the slow dissolution of the alkali-metal metalate complex, which we view as being indicative of the formation of a $\{LiN(SiMe_2CH_2PPr^i_2)_2{\cdot}AER_4\}_x$ (A = Li, Na, E = Al, B, R = Me, Et) type of adduct. In the case of $LiAlEt_4$ (**4**) and $LiBEt_4$ (**5**), the product could only be isolated as a yellow oil; all attempts to generate the adducts as solids failed.

Interestingly, in analogy to **2**, the addition of 4 equiv of EtLi to $AlCl_2[N(SiMe_2CH_2PPr^i_2)_2]$ did not form the same product as the reaction of $LiN(SiMe_2CH_2PPr^i_2)_2$ and $LiAlEt_4$; we only observed the formation of $AlEt_2[N(SiMe_2CH_2PPr^i_2)_2]$.[39] It is probable that the larger ethyl group is unable to effectively insert into the aluminum−amide bond as we propose is likely for the smaller methyl derivative.

(42) Fryzuk, M. D.; Huang, L.; McManus, N. T.; Paglia, P.; Rettig, S. J.; White, G. S. *Organometallics* **1992**, *11*, 2979.

The ^{1}H NMR spectra of **4** and **5** are as expected, with no coupling to lithium present in any of the resonances, as is the case for **2**. The ethyl resonances in **3** remain a triplet ($-CH_2CH_3$) and quartet ($-CH_2CH_3$) even at -90 °C (C_7D_8) and point to the same rapid tumbling behavior on the NMR time scale as was found for the $^-AlMe_4$ group in **2**. The broadened ethyl resonances in **5** are the result of the close proximity of the ethyl groups of the $^-BEt_4$ unit to both the quadrupolar lithium and boron atoms. The singlets in the $^{31}P\{^1H\}$ and $^7Li\{^1H\}$ NMR spectra, in spite of these broadened ^{1}H NMR signals, are further evidence of the dynamic nature of these adducts. Even though we could not obtain these compounds as solids, the uptake of $LiAlEt_4$ and $LiBEt_4$ by toluene solutions of LiN(SiMe$_2$CH$_2$PPr$^i_2$)$_2$ as well as the donation of the amide lone pair to an additional lithium atom in the structures of both **1** and **2** point toward the existence of the adducts **4** and **5**. However, in the absence of structural confirmation, we did not attempt variable-temperature $^{31}P\{^1H\}$ or $^7Li\{^1H\}$ NMR spectroscopic studies of these species.

The addition of LiN(SiMe$_2$CH$_2$PPr$^i_2$)$_2$ to a toluene slurry of $NaBEt_4$ resulted in a yellow oil, the ^{1}H NMR of which was similar to that of **5** in that many of the alkyl resonances were greatly broadened, even with ^{11}B decoupling (eq 2). As for **2**−**5**, the $^{31}P\{^1H\}$ NMR was of

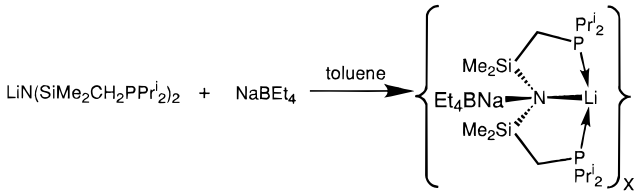

(2)

no use in establishing the formation of an adduct, although the solvation of $NaBEt_4$ upon addition of ligand solution was again positive evidence in this regard. In this case, crystals were isolated which allowed us to further probe the extent and nature of this interaction.

Structure of {LiN(SiMe$_2$CH$_2$PPr$^i_2$)$_2$·NaBEt$_4$}$_x$ (6). Evaporation of a saturated toluene solution of **6** resulted in large colorless plates that were suitable for single-crystal X-ray diffraction. The molecular structure and numbering scheme are illustrated in Figure 6. The structure is best described as being a loosely associated one-dimensional polymer, the repeating unit of which contains two LiN(SiMe$_2$CH$_2$PPr$^i_2$)$_2$·NaBEt$_4$ fragments. The first $^-$N(SiMe$_2$CH$_2$PPr$^i_2$)$_2$ ligand coordinates to a lithium in a tridentate fashion, such that the metal center maintains a roughly tetrahedral geometry (92.5(4)−128.0(4)°), its coordination sphere completed by a weak interaction with three hydrogens on a neighboring $[BEt_4]^-$ anion (Li(2)−H(124*,125*,126*) = 2.27−2.34 Å). The stereochemical importance of achieving coordinative saturation at an electron-deficient metal center via metal−alkane hydrogen interactions has long been known.[43] The bond lengths from the lithium atom to the $^-$N(SiMe$_2$CH$_2$PPr$^i_2$)$_2$ ligand are similar to those determined for **1** and **2**. As in the structures previously discussed, the amide nitrogen is more tetrahedral than planar, owing to the donation of

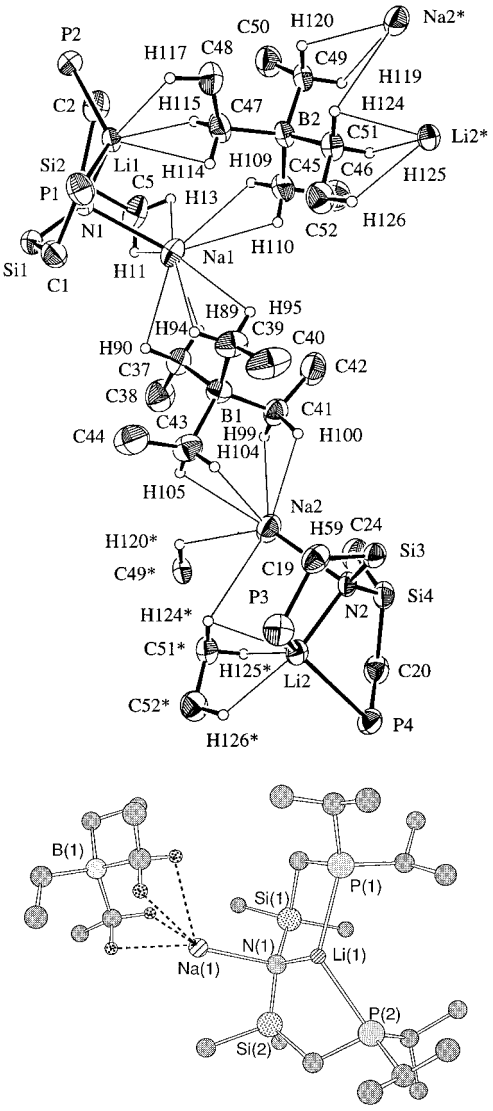

Figure 6. (a, top) Molecular structure of {LiN(SiMe$_2$CH$_2$PPr$^i_2$)$_2$·NaBEt$_4$}$_x$ (**6**; 33% probability thermal ellipsoids are shown). Hydrogen atoms are omitted for clarity. (b, bottom) Chem 3D view of the monomer unit of {LiN(SiMe$_2$CH$_2$PPr$^i_2$)$_2$·NaBEt$_4$}$_x$.

electrons to an alkali metal, in this case sodium. The N(2)−Na(2) distance of 2.447 Å is ∼0.43 Å longer than the distance from this nitrogen to Li(2). The sodium atom serves to bridge the LiN(SiMe$_2$CH$_2$PPr$^i_2$)$_2$ and $[BEt_4]^-$ units via ion−dipole interactions with the four methylene protons of two ethyl groups of the $[BEt_4]^-$ group. These bond distances range from 2.44 to 2.59 Å, indicative of the larger atomic radius of Na as compared to Li. Another close contact (2.48 Å) is present between Na(2) and H(120*), which originates from the same $[BEt_4]^-$ group as the initial Li−H contacts. An additional interaction with H(124*) (2.69 Å), which coordinates to Li(2), results in an unusual seven-coordinate sodium ion. The central $[BEt_4]^-$ group exhibits local C_{2v} symmetry and is normal in terms of usual borate geometries.[44] This general scheme is then repeated in reverse to yield a LiN(SiMe$_2$CH$_2$PPr$^i_2$)$_2$−Na−BEt$_4$−Na−LiN(SiMe$_2$CH$_2$PPr$^i_2$)$_2$ chain. However, the second sodium atom differs from the first in that it is now nine-coordinate. In addition to interactions with

(43) Rhine, W. E.; Stucky, G.; Peterson, S. W. *J. Am. Chem. Soc.* **1975**, *97*, 6401.

(44) Fryzuk, M. D.; Lloyd, B. R.; Clentsmith, G. K. B.; Rettig, S. J. *J. Am. Chem. Soc.* **1994**, *116*, 3804.

Table 4. Selected Bond Lengths (Å) and Angles (deg) for $\{LiN(SiMe_2CH_2PPr^i_2)_2 \cdot NaBEt_4\}_x$ (6)[a]

Na(1)−H(90)	2.47	Na(1)−H(11)	2.63
Na(1)−H(89)	2.46	Na(1)−H(94)	2.49
Na(1)−H(13)	2.64	Na(1)−H(109)	2.69
Na(1)−H(95)	2.44	Na(1)−H(110)	2.62
Na(1)−N(1)	2.431(5)	Na(2)−H(120)*	2.48
Na(2)−N(2)	2.447(5)	Na(2)−H(105)	2.53
Na(2)−H(59)	2.52	Na(2)−H(99)	2.44
Na(2)−H(104)	2.59	Na(2)−H(100)	2.41
Na(2)−H(119)*	2.73	Na(2)−H(124)*	2.69
Li(1)−H(114)	2.41	Li(1)−H(115)	2.12
Li(1)−H(117)	2.35	Li(2)−H(125)*	2.23
Li(2)−H(126)*	2.27	Li(2)−H(124)*	2.34
Si(1)−N(1)	1.701(5)	Si(2)−N(1)	1.700(5)
Si(3)−N(2)	1.693(5)	Si(4)−N(2)	1.690(5)
P(1)−Li(1)	2.57(1)	P(2)−Li(1)	2.60(1)
P(3)−Li(2)	2.59(1)	P(4)−Li(2)	2.60(1)
N(1)−Li(1)	2.05(1)	N(2)−Li(2)	2.03(1)
P(1)−Li(1)−P(2)	136.1(4)	P(1)−Li(1)−N(1)	94.9(4)
P(2)−Li(1)−N(1)	92.7(4)	P(3)−Li(2)−P(4)	128.0(4)
P(3)−Li(2)−N(2)	96.2(5)	P(4)−Li(2)−N(2)	92.5(4)
Na(1)−N(1)−Li(1)	95.8(3)	Na(2)−N(2)−Li(2)	92.9(3)
N(1)−Si(1)−C(1)	107.6(3)	N(1)−Si(1)−C(3)	116.0(3)
N(1)−Si(1)−C(4)	115.6(3)	N(1)−Si(2)−C(2)	110.2(3)
N(1)−Si(2)−C(5)	112.2(3)	N(1)−Si(2)−C(6)	117.4(3)
N(2)−Si(3)−C(19)	107.8(3)	N(2)−Si(3)−C(21)	116.1(3)
N(2)−Si(3)−C(22)	115.6(3)	N(2)−Si(4)−C(20)	110.1(3)
N(2)−Si(4)−C(23)	116.7(3)	N(2)−Si(4)−C(24)	112.3(3)
Si(1)−N(1)−Li(1)	110.0(4)	Si(1)−N(1)−Si(2)	124.3(3)
Si(2)−N(1)−Na(1)	98.9(2)	Si(2)−N(1)−Li(1)	111.1(4)
Si(3)−N(2)−Si(4)	125.1(3)	Si(3)−N(2)−Na(2)	110.9(3)
Si(3)−N(2)−Li(2)	110.8(4)	Si(4)−N(2)−Na(2)	101.4(2)
Si(4)−N(2)−Li(2)	110.5(4)	H(11)−Na(1)−H(90)	71.5

[a] Asterisks denote the symmetry operation $-1 + x, y, z$.

the methylene protons as seen for Na(2), Na(1) now shares not only the electrons of N(1) from the second $^-N(SiMe_2CH_2PPr^i_2)_2$ ligand, but also those of two hydrogens from a third $[BEt_4]^-$ unit in addition to two silyl methyl protons arising from the ligand system, although the increased bond lengths point to a weaker interaction than for the $[BEt_4]^-$ methylene protons. The geometry of the second $LiN(SiMe_2CH_2PPr^i_2)_2$ ligand is similar to that of the first, the most notable exception being the increased P−Li−P angle of 136.1(4)°. As before, the second lithium fulfills its coordination sphere with the three donors of the tridentate ligand and three ion−dipole interactions with neighboring $[BEt_4]^-$ hydrogens. The overall structure of **6** may best be viewed as $\{LiN(SiMe_2CH_2PPr^i_2)_2-Na-BEt_4-Na-LiN(SiMe_2CH_2PPr^i_2)_2\}^+$ chains bridged perpendicularly by $[BEt_4]^-$ groups.[45,46] Notably, the "bridging" $[BEt_4]^-$ units differ from the "chain" $[BEt_4]^-$ groups in that the former coordinate to two lithium atoms as well as two sodium atoms, whereas the latter only interact with two sodium atoms. It is clear from examination of the crystal determination that this structure is held together by predominantly ion−dipole interactions and the donation of electrons from the $^-N(SiMe_2CH_2PPr^i_2)_2$ ligand amide lone pairs to adjacent sodium ions. A partial list of bond lengths and bond angles for **6** is presented in Table 4.

The polymeric nature of **6** is most likely the result of aggregation upon solvent evaporation; in other words, this structure is not maintained in solution. The solution molecular weight of this compound (Signer method), which corresponds to a simple 1:1 adduct of $LiN(SiMe_2CH_2PPr^i_2)_2$ and $NaBEt_4$, and the decreased ease with which crystals of this compound can be redissolved after isolation are further proof of the polymeric nature of **6** in the solid form, but the simple monomeric form that **6** maintains in solution. We did not probe the nature of this interaction by variable-temperature NMR spectroscopy any further.

Similarity of Ligand Geometry and Trends in Adduct Formation. Although the crystal structure of $LiN(SiMe_2CH_2PPr^i_2)_2$ still remains elusive, we have been able to isolate three adducts of our ligand system in which three different modes of coordination are observed: a three-rung ladder with LiCl, a 2:2 dimer with $LiAlMe_4$, and an infinite one-dimensional polymer with $NaBEt_4$. It may be that the degree of aggregation depends upon the size of the anion present: ^-Cl (three-rung ladder) < $^-AlMe_4$ (2:2 dimer) < $^-BEt_4$ (polymer). The presence of the counteranion in these complexes determines the amount of steric crowding around the corresponding alkali metal and undoubtedly the final stoichiometry. What is striking is the remarkable similarity in the geometry of the $LiN(SiMe_2CH_2PPr^i_2)_2$ unit in the face of varying coordination modes (see Tables 5 and 6). With the exception of the small variations in Li−P bond lengths and the P−Li−P bond angles, the geometric parameters can be said to be identical within experimental error.

Conclusions

Adducts of the lithium salt of the potentially ancillary, potentially tridentate ligand precursor $LiN(SiMe_2CH_2PPr^i_2)_2$ were synthesized by the addition of the suitable lithium or sodium "ate" species to $LiN(SiMe_2CH_2PPr^i_2)_2$. The solution structures of these compounds are postulated to be highly fluxional, on the basis of their variable-temperature heteronuclear NMR spectroscopic properties. The solid-state structures of these compounds were found to vary from those found in solution; the exception is the three-rung-ladder lithium chloride adduct **1**, for which the solution data indicate a similar structure to that in the solid state.

Experimental Section

Procedures. Unless otherwise stated, all manipulations were performed under an atmosphere of dry, oxygen-free dinitrogen or argon by means of standard Schlenk or glovebox techniques. The glovebox used was a Vacuum Atmospheres HE-553-2 model equipped with a MO-40-2H purification system and a −40 °C freezer. ^1H, $^{31}P\{^1H\}$, $^{29}Si\{^1H\}$, $^{15}N\{^1H\}$, $^7Li\{^1H\}$, and $^6Li\{^1H\}$ NMR spectroscopy was performed on a Varian XL-300 spectrometer operating at 299.9, 121.4, 59.9, 30.3, 116.7, and 44.1 MHz, respectively. ^1H NMR spectra were referenced to internal C_6D_5H (7.15 ppm) or $C_6D_5CD_2H$ (2.09 ppm). $^{31}P\{^1H\}$ NMR spectra were referenced to external $P(OMe)_3$ (141.0 ppm with respect to 85% H_3PO_4 at 0.0 ppm). $^{29}Si\{^1H\}$ NMR spectra were referenced to external hexamethyldisiloxane in C_7D_8 (0.00 ppm). $^{15}N\{^1H\}$ NMR spectra were referenced to external $^{15}NH_4Cl$ in D_2O (0.00 ppm). The references for the $^7Li\{^1H\}$ and $^6Li\{^1H\}$ NMR spectra were ^7LiCl and ^6LiCl, respectively (0.00 ppm), in D_2O. The ^7Li NOESY spectrum was obtained on a Bruker AMX-500 instrument operating at 194.4 MHz in C_7D_8 at 223 K; t_1 was incremented in 512 steps, and the data were zero-filled to 1024 words before Fourier transformation. Sixteen scans were recorded for each increment with $t_{mix} = 5$ or 50 ms with a relaxation time of 800 ms. Simulations of the variable-temperature ^7Li and ^6Li

(45) Barr, D.; Snaith, R.; Mulvey, R. E.; Perkins, P. G. *Polyhedron* **1988**, *7*, 2119.
(46) Gerteis, R. L.; Dickerson, R. E.; Brown, T. L. *Inorg. Chem.* **1964**, *3*, 872.

Table 5. Selected Bond Lengths (Å) in {LiN(SiMe$_2$CH$_2$PPr$^i_2$)$_2$}$_2$LiCl (1), {LiN(SiMe$_2$CH$_2$PPr$^i_2$)$_2$·LiAlMe$_4$}$_2$ (2), and {LiN(SiMe$_2$CH$_2$PPr$^i_2$)$_2$·NaBEt$_4$}$_x$ (6)

ligand bond length	1	2	6
Li-N	2.06(1), 2.10(1)	2.075(8)	2.05(1), 2.03(1)
Li-P	2.59(1), 2.63(1)	2.538(7), 2.675(7)	2.57(1), 2.60(1)
	2.61(1), 2.58(1)		2.59(1), 2.60(1)
N-Si	1.702(4), 1.687(5)	1.698(3), 1.707(3)	1.701(5), 1.700(5)
	1.702(5), 1.694(4)		1.693(5), 1.690(5)

Table 6. Selected Bond Angles (deg) in {LiN(SiMe$_2$CH$_2$PPr$^i_2$)$_2$}$_2$LiCl (1), {LiN(SiMe$_2$CH$_2$PPr$^i_2$)$_2$·LiAlMe$_4$}$_2$ (2), and {LiN(SiMe$_2$CH$_2$PPr$^i_2$)$_2$·NaBEt$_4$}$_x$ (6)

ligand bond angles	1	2	6
P−Li−P	117.9(4), 118.9(4)	124.1(3)	136.1(4), 128.0(4)
P−Li−N	97.1(4), 96.5(4)	96.9(3), 96.3(3)	94.9(4), 92.7(4)
	97.0(4), 95.5(4)		96.2(5), 92.5(4)
Li−N−Si	107.2(4), 110.7(4)	109.9(2), 104.8(2)	110.0(4), 111.1(4)
	107.3(3), 110.1(3)		110.8(5), 110.5(4)

spectra were performed by DNMR-SIM. Microanalyses (C, H, N) were performed by Mr. P. Borda of this department.

Materials. LiN(SiMe$_2$CH$_2$PPr$^i_2$)$_2$,[26] AlCl$_2$N(SiMe$_2$CH$_2$PPr$^i_2$)$_2$,[39] and LiPPr$^i_2$[26] were prepared by published procedures. Li^{15}N(SiMe$_2$CH$_2$PPr$^i_2$)$_2$ and AlCl$_2$^{15}N(SiMe$_2$CH$_2$PPr$^i_2$)$_2$ were prepared in a fashion analogous to their ^{14}N congeners from the starting labeled disilazane H^{15}N(SiMe$_2$CH$_2$Cl)$_2$.[47] MeLi (1.4 M solution in ether) was purchased from Aldrich and used as received. Me^{6}Li was prepared by the addition of CH$_3$Cl to an ethereal ^{6}Li solution.[48] LiAlMe$_4$ was prepared by the addition of MeLi to a toluene solution of AlMe$_3$. LiAlEt$_4$ and LiBEt$_4$ were prepared in a similar manner with EtLi and either AlEt$_3$ or BEt$_3$.[46,49] NaBEt$_4$ was obtained from Strem and used without further purification.

Hexanes, toluene, THF, and Et$_2$O were refluxed over CaH$_2$ prior to a final distillation from either sodium metal or sodium benzophenone ketyl under an Ar atmosphere. Deuterated solvents were dried by distillation from sodium benzophenone ketyl; oxygen was removed by three freeze−pump−thaw cycles.

{LiN(SiMe$_2$CH$_2$PPr$^i_2$)$_2$}$_2$LiCl (1). To a solution of HN(SiMe$_2$CH$_2$Cl)$_2$ (1.73 g, 7.51 mmol) in 20 mL of THF was added a 20 mL THF solution of LiPPr$^i_2$ (2.92 g, 23.5 mmol) at −78 °C, dropwise. The solution was stirred and warmed to room temperature overnight. The THF was then removed *in vacuo* and the residue extracted with hexanes (3 × 20 mL). After filtration through Celite to remove LiCl, the hexanes were removed to yield an orange oil (2.21 g; 70% yield). This was then taken up in a minimum volume of hexanes and cooled to −40 °C. Large blocks formed upon standing for 2 weeks. ^{1}H NMR (C$_6$D$_6$): δ 1.76 (d of sept, 4H, C*H*Me$_2$, $^3J_{H-H}$ = 6.5 Hz, $^2J_{H-P}$ = 3.1 Hz), 1.11 and 1.06 (dd, 24H, CH*MeMe*′, $^3J_{H-H}$ = 6.5 Hz, $^3J_{H-P}$ = 5.0 Hz), 0.73 (br d, 4H, C*H*$_2$P, $^2J_{H-P}$ = 5.5 Hz), 0.45 (s, 12H, Si*Me*$_2$). ^{31}P{^{1}H} NMR (C$_6$D$_6$, 20 °C): δ −3.8 (s, 490 Hz peak width at half-height). ^{31}P{^{1}H} NMR (C$_7$D$_8$, −27 °C): δ −6.2 (1:1:1:1 q, $^1J_{P-Li}$ = 48.5 Hz). ^{7}Li{^{1}H} NMR (C$_6$D$_6$, 20 °C): δ −0.7 (s, 50 Hz peak width at half-height). ^{7}Li{^{1}H} (C$_7$D$_8$, −38 °C): δ −0.4 (t, 2Li, $^1J_{Li-P}$ = 48.5 Hz), −1.4 (br s, 1Li, 110 Hz peak width at half-height). ^{15}N{^{1}H} NMR (C$_7$D$_8$): δ 5.1 (s). ^{29}Si{^{1}H} NMR (C$_7$D$_8$): δ −17.2 (s, 40 Hz peak width at half-height). Anal. Calcd for C$_{36}$H$_{88}$ClLi$_3$N$_2$P$_4$Si$_4$: C, 51.38; H, 10.54; N, 3.33. Found: C, 51.13; H, 10.41; N, 3.50.

{LiN(SiMe$_2$CH$_2$PPr$^i_2$)$_2$·LiAlMe$_4$}$_2$ (2). Method 1. To a 10 mL toluene solution of AlCl$_2$N(SiMe$_2$CH$_2$PPr$^i_2$)$_2$ (204 mg, 0.416 mmol) was added MeLi (1.20 mL of a 1.4 M solution, diluted with 10 mL of ether, 1.68 mmol) dropwise at room temperature. The solution immediately turned cloudy white. The reaction mixture was then stirred for 3 h, after which time it was filtered through a frit lined with Celite to remove LiCl. The solvent was then removed *in vacuo* to yield **2** as a clear colorless oil. This was then taken up in a minimum amount of toluene. Slow evaporation afforded **2** as colorless plates (94 mg; 46% yield).

Method 2. LiAlMe$_4$ (23 mg, 0.245 mmol) was slurried in approximately 10 mL of toluene. To this was added a toluene solution (10 mL) of LiN(SiMe$_2$CH$_2$PPr$^i_2$)$_2$ (101 mg, 0.253 mmol). Upon addition, the LiAlMe$_4$ slowly dissolved until only a clear solution remained. The reaction mixture was then stirred for 2 h, after which time the solvent was removed *in vacuo*. The resulting clear, colorless oil was taken up in a minimum amount of toluene. Slow evaporation of the solvent resulted in the deposition of colorless plates (96 mg; 71% yield). ^{1}H NMR (C$_6$D$_6$): δ 1.54 (d of sept, 4H, C*H*MeMe′, $^3J_{H-H}$ = 7.3 Hz, $^2J_{H-P}$ = 3.9 Hz), 0.93 and 0.88 (dd, 24H, CH*MeMe*′, $^3J_{H-H}$ = 7.3 Hz, $^3J_{H-P}$ = 6.5 Hz), 0.49 (d, 4H, C*H*$_2$P, $^2J_{H-P}$ = 7.8 Hz), 0.21 (s, 12H, Si*Me*$_2$), −0.21 (s, 12H, Al*Me*$_4$). ^{1}H NMR (THF-*d*$_8$): δ 1.71 (d of sept, 4H, C*H*Me$_2$, $^3J_{H-H}$ = 7.6 Hz, $^2J_{H-P}$ = 2.5 Hz), 1.05 (dd, 24H, CH*MeMe*′, $^3J_{H-H}$ = 7.6 Hz, $^3J_{H-P}$ = 4.6 Hz), 0.47 (d, 4H, C*H*$_2$P, $^2J_{H-P}$ = 5.0 Hz), −0.05 (s, 12H, Si*Me*$_2$), −1.36 (1:1:1:1:1:1 sext, 12H, Al*Me*$_4$, $^2J_{H-Al}$ = 6.1 Hz). ^{31}P{^{1}H} NMR (C$_7$D$_8$, 20 °C): δ −3.5 (s). ^{31}P{^{1}H} NMR (−88 °C): δ −8.6 (s). ^{31}P{^{1}H} NMR (THF-*d*$_8$, 20 °C): δ −0.3 (s). ^{6}Li{^{1}H} NMR (C$_7$D$_8$, 20 °C): δ 1.4 (s). ^{6}Li{^{1}H}NMR (C$_7$D$_8$/pentane, −48 °C): δ 1.2 (t of d, $^1J^6_{Li-P}$ = 10.8 Hz, $^1J^6_{Li-^{15}N}$ = 3.2 Hz). ^{6}Li{^{1}H}NMR (−108 °C): δ 1.9 (t of d, 1Li, $^1J^6_{Li-P}$ = 19.9 Hz, $^1J^6_{Li-^{15}N}$ = 2.0 Hz), 0.7 (d, 1Li, $^1J^6_{Li-^{15}N}$ = 4.0 Hz). ^{6}Li{^{1}H} NMR (THF-*d*$_8$, 20 °C): δ 0.1 (s). ^{15}N{^{1}H} NMR (C$_7$D$_8$): δ 27.3 (s). ^{29}Si{^{1}H} NMR (C$_7$D$_8$): δ −18.5 (s). Mol wt (Signer, isopiestic method, toluene): found, 430 ± 40; calcd, 493.67. Anal. Calcd for C$_{22}$H$_{56}$AlLi$_2$NP$_2$Si$_2$: C, 53.53; H, 11.43; N, 2.84. Found: C, 52.67; H, 11.10; N, 2.90.

LiN(SiMe$_2$CH$_2$PPr$^i_2$)$_2$·AlMe$_3$ (3). To a 10 mL toluene solution of AlCl$_2$N(SiMe$_2$CH$_2$PPr$^i_2$)$_2$ (200 mg, 0.408 mmol) was added MeLi (0.87 mL of a 1.4 M solution, diluted with 10 mL of ether, 1.22 mmol) dropwise at room temperature. The solution immediately turned cloudy white. The reaction mixture was then stirred for 3 h, after which time it was filtered through a frit lined with Celite to remove LiCl. The solvent was then removed *in vacuo* to yield **2** as a clear colorless oil (123 mg; 64% yield). This species was only analyzed in solution. ^{1}H NMR (C$_6$D$_6$): δ 1.56 (d of sept, 4H, C*H*Me$_2$, $^3J_{H-H}$ = 7.8 Hz, $^2J_{H-P}$ = 3.4 Hz), 0.94 and 0.89 (dd, 24H, CH*MeMe*′, $^3J_{H-H}$ = 7.8 Hz, $^3J_{H-P}$ = 6.4 Hz), 0.51 (d, 4H, C*H*$_2$P, $^2J_{H-P}$ = 7.3 Hz), 0.23 (s, 12H, Si*Me*$_2$), −0.30 (s, 9H, Al*Me*$_3$). ^{31}P{^{1}H} NMR (C$_6$D$_6$): δ −4.0 (s). ^{7}Li{^{1}H} NMR (C$_6$D$_6$): δ −0.9 (s). Mol wt (Signer, isopiestic method, toluene): found, 450 ± 40; calcd, 471.70.

LiN(SiMe$_2$CH$_2$PPr$^i_2$)$_2$·LiAlEt$_4$ (4). LiAlEt$_4$ (113 mg, 0.752 mmol) was slurried in approximately 10 mL of toluene. To this was added a toluene solution (10 mL) of LiN(SiMe$_2$CH$_2$PPr$^i_2$)$_2$ (300 mg, 0.751 mmol). Upon addition, the LiAlEt$_4$ slowly dissolved until only a clear solution remained. The reaction mixture was stirred for 2 h, after which time the

(47) Fryzuk, M. D.; MacNeil, P. A. *J. Am. Chem. Soc.* **1984**, *106*, 6993.
(48) Schlosser, M. *Organometallics in Synthesis*; Wiley: West Sussex, U.K., 1994; p 603.
(49) Honeycutt, J. B.; Riddle, J. M. *J. Am. Chem. Soc.* **1961**, *83*, 369.

solvent was removed *in vacuo*, resulting in a yellow oil (384 mg; 84% yield). Purification by recrystallization was not possible either due to the compound's extreme solubility in hydrocarbon solvents or because it was low melting; as a result, characterization by elemental analysis was not possible. ^{1}H NMR (C_6D_6): δ 1.58 (d of sept, 4H, C*H*Me$_2$, $^3J_{H-H}$ = 8.3 Hz, $^2J_{H-P}$ = 3.6 Hz), 1.49 (t, 12H, AlCH$_2$C*H*$_3$, $^3J_{H-H}$ = 7.9 Hz), 0.96 and 0.90 (dd, 24H, CH*MeMe*′, $^3J_{H-H}$ = 8.3 Hz, $^3J_{H-P}$ = 4.0 Hz), 0.51 (d, 4H, C*H*$_2$P, $^2J_{H-P}$ = 7.1 Hz), 0.19 (s, 12H, Si*Me*$_2$), 0.03 (q, 8H, AlC*H*$_2$CH$_3$, $^3J_{H-H}$ = 7.9 Hz). ^{31}P{^{1}H} NMR (C_6D_6): δ −3.6 (s). ^{7}Li{^{1}H} NMR (C_6D_6): δ −1.3 (s).

LiN(SiMe$_2$CH$_2$PPr$^i_2$)$_2$·LiBEt$_4$ (5). LiBEt$_4$ (100 mg, 0.746 mmol) was slurried in approximately 10 mL of toluene. To this was added a toluene solution (10 mL) of LiN(SiMe$_2$CH$_2$PPr$^i_2$)$_2$ (300 mg, 0.751 mmol). The reaction mixture was then stirred for 2 h, after which time the solvent was removed *in vacuo*, resulting in a yellow oil (364 mg; 81% yield). Purification by recrystallization was not possible either due to the compound's extreme solubility in hydrocarbon solvents or because it was low melting; as a result, characterization by elemental analysis was not possible. ^{1}H NMR (C_6D_6): δ 1.60 (d of sept, 4H, C*H*Me$_2$, $^3J_{H-H}$ = 7.3 Hz, $^2J_{H-P}$ = 2.9 Hz), 1.39 (br t, 12H, BCH$_2$C*H*$_3$, $^3J_{H-H}$ = 7.7 Hz), 0.98 and 0.91 (mult, 24H, CH*MeMe*′, $^3J_{H-H}$ = 7.3 Hz), 0.64 (d, 4H, C*H*$_2$P, $^2J_{H-P}$ = 7.2 Hz), 0.58 (mult, 8H, BC*H*$_2$CH$_3$), 0.29 (s, 12H, Si*Me*$_2$). ^{31}P{^{1}H} NMR (C_6D_6): δ −4.0 (s). ^{7}Li{^{1}H} NMR (C_6D_6): δ −1.4 (s).

{LiN(SiMe$_2$CH$_2$PPr$^i_2$)$_2$·NaBEt$_4$}$_x$ (6). NaBEt$_4$ (40 mg, 0.274 mmol) was slurried in approximately 10 mL of toluene. To this was added a toluene solution (10 mL) of LiN(SiMe$_2$CH$_2$PPr$^i_2$)$_2$ (105 mg, 0.263 mmol). Upon addition, the NaBEt$_4$ slowly dissolved until only a clear solution remained. The reaction mixture was then stirred a further 12 h, after which time the solvent was removed *in vacuo*. The resulting yellow oil was taken up in a minimum amount of toluene. Slow evaporation of the solvent resulted in the deposition of colorless plates (91 mg; 60% yield). ^{1}H NMR (C_6D_6): δ 1.60 (d of sept, 4H, C*H*Me$_2$, $^3J_{H-H}$ = 7.0 Hz, $^2J_{H-P}$ = 2.1 Hz), 1.38 (br t, 12H, BCH$_2$C*H*$_3$), 1.00 and 0.91 (dd, 24H, CH*MeMe*′, $^3J_{H-H}$ = 7.0 Hz, $^3J_{H-P}$ = 5.2 Hz), 0.56 (d, 4H, C*H*$_2$P, $^2J_{H-P}$ = 5.0 Hz), 0.38 (br q, 8H, BC*H*$_2$CH$_3$), 0.19 (s, 12H, Si*Me*$_2$). ^{31}P{^{1}H} NMR (C_6D_6): δ −4.2 (s). Mol wt (Signer, isopiestic method, toluene): found, 520 ± 50; calcd, 549.67. Anal. Calcd for $C_{22}H_{56}BLiNNaP_2Si_2$: C, 56.81; H, 11.74; N, 2.55. Found: C, 57.21; H, 11.74; N, 2.41.

X-ray Crystallographic Analyses of {LiN(SiMe$_2$CH$_2$PPr$^i_2$)$_2$}$_2$LiCl (1), {LiN(SiMe$_2$CH$_2$PPr$^i_2$)$_2$·LiAlMe$_4$}$_2$ (2), and {LiN(SiMe$_2$CH$_2$PPr$^i_2$)$_2$·NaBEt$_4$}$_x$ (6). Crystallographic data appear in Table 1. The final unit-cell parameters were obtained by least squares on the setting angles for 25 reflections with 2θ = 30.4−41.4° for **1**, 55.1−63.2° for **2**, and 25.3−39.2° for **6**. The intensities of three standard reflections, measured every 200 reflections throughout the data collections, decayed linearly for **1** (6.5%), **2** (9.3%), and **6** (5.2%). The data were processed[50] and corrected for Lorentz and polarization effects, decay, and absorption (empirical, based on azimuthal scans).

The structures were solved by direct methods. The structure analysis of **2** was initiated in the centrosymmetric space group $P\bar{1}$, this choice being confirmed by subsequent calculations. There are two formula units in the asymmetric unit of **6**, which exists in the solid state as a weakly associated polymer. The low-occupancy carbon atoms C(12a), C(18a), and C(35a) in **1** were refined isotropically, while all remaining nonhydrogen atoms were refined with anisotropic thermal parameters. Three isopropyl groups in **1** and one isopropyl group in **2** had disordered terminal carbon atoms—these were modeled by split-atom refinement. The minor-component H atoms of the C(34−36) isopropyl group in **1**, which has a more complex disorder, and the disordered methine H bound to C(31) in **2** were not included in the models. The remaining hydrogen atoms in **1**, **2**, and **6** were fixed in calculated positions with C−H = 0.98 Å and $B_H = 1.2B_{\text{bonded atom}}$. Secondary extinction corrections were applied in each refinement (Zachariasen type 1 isotropic), the final values of the extinction coefficients being [2.12(12)] × 10^{-6} for **1**, [1.03(5)] × 10^{-6} for **2**, and [1.67(14)] × 10^{-7} for **6**. Neutral atom scattering factors and anomalous dispersion corrections were taken from the ref 51.

Selected bond lengths and bond angles appear in Tables 2−4. Tables of final atomic coordinates and equivalent isotropic thermal parameters, anisotropic thermal parameters, bond lengths and angles, torsion angles, intermolecular contacts, and least-squares planes are included as Supporting Information.

Acknowledgment. Financial support was generously provided by the NSERC of Canada in the form of grants to M.D.F. and a postgraduate scholarship to G.R.G. We thank Dr. N. E. Burlinson for help in acquiring the ^{7}Li NOESY data. We also acknowledge the helpful comments of a reviewer.

Supporting Information Available: Complete tables of bond lengths and bond angles, final atomic coordinates, hydrogen atom parameters, anisotropic thermal parameters, torsion angles, intermolecular contacts, and least-squares planes for **1**, **2**, and **6** (102 pages). Ordering information is given on any current masthead page.

OM960638C

(50) teXsan: Crystal structure analysis package; Molecular Structure Corp., The Woodlands, TX, 1985 and 1992.

(51) (a) *International Tables for X-Ray Crystallography*; Kynoch Press: Birmingham, U.K. (present distributor Kluwer Academic: Boston, MA), 1974; Vol. IV, pp 99−102; (b) *International Tables for Crystallography*; Kluwer Academic: Boston, MA, 1992; Vol. C, pp 200−206.